EPJ Web of Conferences **303**, 01016 (2024) https://doi.org/10.1051/epjconf/202430301016
MENU 2023

Combination of Bayesian inference with truncated partial-wave analysis

Philipp Kroenert[1,*], *Yannick* Wunderlich[1], *Farah* Afzal[1], and *Annika* Thiel[1]

[1]Helmholtz Institut für Strahlen- und Kernphysik, Universität Bonn, Germany

Abstract. This work combines experimental data from baryon spectroscopy with the latest statistical analysis-methods. The results are model-independent estimates of electromagnetic multipole parameters from which model-independent predictions of yet unmeasured polarization observables were calculated for the reaction $\gamma p \rightarrow \eta p$, slightly above production threshold. For this purpose, truncated partial-wave analysis is combined with Bayesian inference for the first time. Thus, all results are given as distributions in contrast to point-estimates, which allows for an unprecedented uncertainty estimation.

1 Introduction

Baryon spectroscopy studies the excitation spectrum of baryons, i.e. so-called resonance states. The measurable quantities of interest are polarization observables. In the case of pseudoscalar-meson photoproduction, for example the reaction $\gamma p \rightarrow \eta p$, sixteen polarization observables can be measured via different polarization configurations for beam, target- and recoil baryon [1], see also Table 2.

Partial-wave analysis (PWA) utilizes polarization observables as input for a regression analysis to determine additional physical information about the photoproduction reaction of interest. The extracted information ranges from determining resonance parameters (total angular momentum, parity, mass, etc.), to predicting yet unmeasured polarization observables. Examples for PWA's are Bonn-Gatchina (K-Matrix) [2], Jülich-Bonn (dynamical coupled-channel) [3] and Eta-MAID (unitarized isobar-model) [4]. However, these PWA approaches rely on an energy dependent parameterization for the complex spin amplitudes [5], which makes the results model dependent. In contrast, truncated partial-wave analysis (TPWA) is a straightforward yet model-independent approach. For an introduction to TPWA see Ref. [6].

Within the present work, the six polarization observables $\sigma_0, \Sigma, T, E, F$ and G of η-photoproduction off the proton were utilized as input for a TPWA. An overview is given in Table 1. This combination of observables was carefully selected to ensure that no ambiguities, except so-called 'accidental' ambiguities which can not be avoided, are present in the final parameter results. A proof for these claims can be found in Ref. [7].

*e-mail: kroenert@hiskp.uni-bonn.de

© The Authors, published by EDP Sciences. This is an open access article distributed under the terms of the Creative Commons Attribution License 4.0 (https://creativecommons.org/licenses/by/4.0/).

Table 1. Dimensionless polarization observables used for the TPWA of $\gamma p \to \eta p$. The energy and angular ranges are given as intervals. Only a small subset of the data points can be used for TPWA.

Observable	Number of data points	E_γ^{lab} / MeV	$\cos(\theta)$	Facility	References
σ_0	5736	$[723, 1571]$	$[-0.958, 0.958]$	MAMI	Kashevarov et al. [8]
T, F	144	$[725, 1350]$	$[-0.917, 0.917]$	MAMI	Akondi et al. [9]
Σ	140	$[761, 1472]$	$[-0.946, 0.815]$	GRAAL	Bartalini et al. [10]
E	84	$[750, 1350]$	$[-0.917, 0.917]$	MAMI	Afzal et al. [11, 12]
G	47	$[750, 1250]$	$[-0.889, 0.667]$	CBELSA/TAPS	Müller et al. [13]

The fits were performed to data at lab frame photon energies E_γ^{lab} of 750, 850, 950, 1050, 1150 and 1250 MeV for different maximal angular momentum truncation orders $\ell_{\max}$.

2 Statistical model

The statistical framework of Bayes' theorem [14, 15] was used, which can be written as:

$$p(\boldsymbol{\Theta} \mid \mathbf{y}) \propto p(\mathbf{y} \mid \boldsymbol{\Theta})\, p(\boldsymbol{\Theta}), \tag{1}$$

with the posterior distribution $p(\boldsymbol{\Theta} \mid \mathbf{y})$, the likelihood distribution $p(\mathbf{y} \mid \boldsymbol{\Theta})$ and the prior distribution $p(\boldsymbol{\Theta})$. The symbol $\boldsymbol{\Theta}$ represents the parameters of the TPWA and $\mathbf{y}$ stands for the data points of the profile functions of the polarization observables. The profile function of a polarization observable is defined as the observable multiplied with the unpolarized differential cross-section σ_0. Hence, this introduces correlations between certain data points of σ_0 and the profile functions, as well as between the profile functions themselves.

For the likelihood distribution, an N-dimensional multivariate Gaussian distribution is used, the validity of the underlying assumptions is discussed in Ref. [7]:

$$p(\mathbf{y} \mid \boldsymbol{\Theta}) = \mathcal{N}(\boldsymbol{\mu}, \boldsymbol{\Lambda}) = \frac{\exp\left(-\frac{1}{2}(\mathbf{y}-\boldsymbol{\mu})^{\mathrm{T}} \boldsymbol{\Lambda}^{-1} (\mathbf{y}-\boldsymbol{\mu})\right)}{\sqrt{(2\pi)^N |\boldsymbol{\Lambda}|}}, \tag{2}$$

where $\mathbf{y} \in \mathbb{R}^N$ represents the in total N profile function data points. The only input for the predictions of the TPWA model $\boldsymbol{\mu}$ are the angular values at which the $\mathbf{y}$ were measured and the maximal angular momentum $\ell_{\max}$. The covariance matrix $\boldsymbol{\Lambda}$ takes into account the effect of correlated data points on the variance of the parameter estimates. Furthermore, the overall systematic uncertainty for each of the six data sets is taken into account within the analysis through the utilization of nuisance parameters $\boldsymbol{\kappa} \in \mathbb{R}^6$.

The prior distributions for the multipole parameters were chosen conservatively, i.e. relatively uninformative with respect to the likelihood distribution, as uniform distributions with the bounds corresponding to the physically allowed limits of the respective multipole parameter. For the nuisance parameters, a normal distribution with a mean value of one and a variance, which is calculated from the respectively reported systematic uncertainties of the polarization observable measurement, were used.

The fit quality of the applied statistical model can be monitored via so-called posterior predictive checks, for example the Bayesian p-value [15].

3 Results

The results of the analysis are model-independent estimates of electromagnetic multipole parameters. For a TPWA with truncation order $\ell_{\max} = 2$ there are in total fifteen real and imaginary parts of the complex multipole parameters to be determined per analyzed energy. Two examples are shown in Fig. 1. Our results are compared with the PWA results of BnGa-2019 (dotted line) [13], EtaMAID2018 (dashed line) [16] and JüBo-2022 (dash-dotted line) [17]. In the left part of Fig. 1, the imaginary part of the multipole E_{2-} is plotted as a function of the incident photon energy. The contribution of a specific solution, in terms of probability mass, to the posterior is shown with a color range, i.e. from sienna (less relevant) to blue (more relevant). A more detailed plot on the right hand side of Fig. 1 shows the real part of E_{0+}. The upper part of the plot contains point-estimates from a-posteriori estimates, multiple 'accidental' ambiguities of varying relevance are apparent. The middle part shows the marginal parameter distribution. Again, multiple 'accidental' ambiguities are visible as different colored distributions. In the lower part, the log posterior density values are plotted which can be used to compare the relevance of the multiple solutions, i.e. larger values indicate a solution with more relevance for the overall posterior.

The combined data sets show clear D-wave contributions, but do not allow for identification of any contributions from higher partial waves. Due to the large amount of fitting parameters and energies that were fitted, a representative selection of images is shown. More results can be found in Ref. [7].

From the multipole estimates, predictions for all of the not yet measured polarization observables, namely $O_{x'}$, $O_{z'}$, $C_{x'}$, $C_{z'}$, $T_{x'}$, $T_{z'}$, $L_{x'}$ and $L_{z'}$, were calculated. As an example, the predictions for $L_{x'}$ at 950 MeV and $C_{z'}$ at 1250 MeV are shown in Fig. 2. Predicted data distributions, resulting from different 'accidental' ambiguities, are drawn in different colors. Some of these show a significantly different functional behavior over the angular range. These different trends permit, considering all predictions, a selection of promising observables for future measurements in order to remove some or even all 'accidental' ambiguities within the results. Hereby, the observable $C_{z'}$ is a strong candidate for all analyzed energies. For more details see Ref. [7].

4 Summary

A TPWA was conducted for η-photoproduction for six energies slightly above the $p\eta$-production threshold. Model-independent multipole-parameters were estimated, from which all of the not yet measured polarization observables of pseudoscalar meson photoproduction were predicted. Through the utilization of Bayesian inference, the uncertainty for all estimated quantities could be determined with an unprecedented level of accuracy. Although the TPWA approach is not as advanced as the PWA models of BnGa, JüBo and MAID, and despite the fact that far less data could be utilized, the TPWA for η-photoproduction achieved comparable physics results and predictive power.

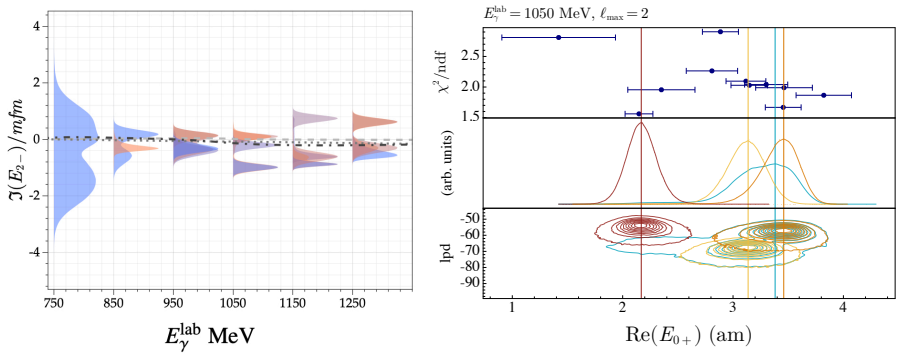

Figure 1. (Left) Electromagnetic Multipole parameter Im(E_{2-}) vs. photon lab energy. The PWA results of BnGa-2019 (dotted line) [13], EtaMAID2018 (dashed line) [16] and JüBo-2022 (dash-dotted line) [17] are shown as well. (Right) Electromagnetic Multipole parameter Re(E_{0+}) at photon lab energy of 1050 MeV (right). The images are sourced from Ref. [7].

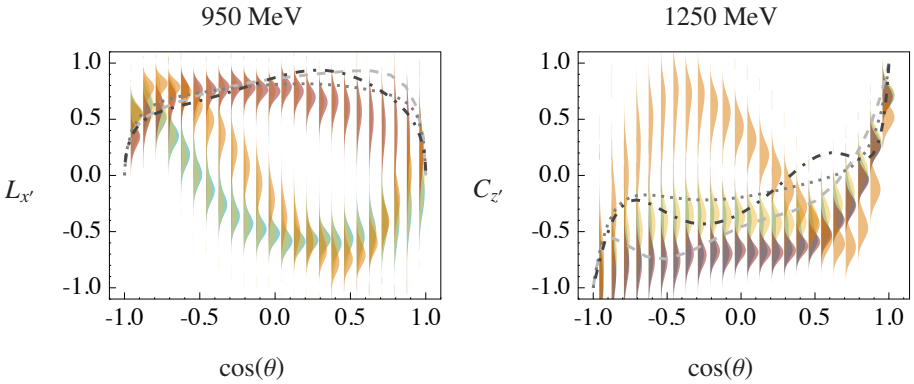

Figure 2. Predicted data distributions for $L_{x'}$ at $E_\gamma^{\rm lab}$ = 950 MeV and $C_{z'}$ at $E_\gamma^{\rm lab}$ = 1250 MeV. The results of BnGa-2019 (dotted line) [13], EtaMAID2018 (dashed line) [16] and JüBo-2022 (dash-dotted line) [17] are shown as well. Each peak of a distribution corresponds to an accidental ambiguity. The images are sourced from Ref. [7].

Table 2. The sixteen polarization observables of pseudoscalar meson photoproduction defined by the required polarization states of beam, target- and recoil baryon. The following statements apply to the center-of-mass frame. The unprimed coordinate system: the positive $\hat{z}$-axis points along the incident photon beam direction. The reaction plane is defined by $\hat{x} - \hat{z}$, where $\hat{y}$ is perpendicular to it. The primed coordinate system: rotation of the unprimed system such that $\hat{z}'$-axis aligns with the direction of the final state meson momentum. The table is redrawn from Ref. [1, 7].

Observable	Beam polarization	Direction of target-/recoil-nucleon polarization
σ_0	unpolarized	—
Σ	linear	—
T	unpolarized	y
P	unpolarized	y'
H	linear	x
P	linear	y
G	linear	z
F	circular	x
E	circular	z
$O_{x'}$	linear	x'
T	linear	y'
$O_{z'}$	linear	z'
$C_{x'}$	circular	x'
$C_{z'}$	circular	z'
$T_{x'}$	unpolarized	x, x'
$L_{x'}$	unpolarized	z, x'
Σ	unpolarized	y, y'
$T_{z'}$	unpolarized	x, z'
$L_{z'}$	unpolarized	z, z'

References

[1] A.M. Sandorfi, S. Hoblit, H. Kamano, T.S.H. Lee, Journal of Physics G: Nuclear and Particle Physics **38**, 053001 (2011)
[2] A. Anisovich, R. Beck, E. Klempt, V. Nikonov, A. Sarantsev, U. Thoma, The European Physical Journal A **48**, 1 (2012)
[3] D. Rönchen, M. Döring, U.G. Meißner, The European Physical Journal A **54**, 1 (2018)
[4] D. Drechsel, O. Hanstein, S. Kamalov, L. Tiator, Nuclear Physics A **645**, 145 (1999)
[5] A. Thiel, F. Afzal, Y. Wunderlich, Progress in Particle and Nuclear Physics **125**, 103949 (2022)
[6] Y. Wunderlich, Ph.D. thesis, Rheinische Friedrich-Wilhelms-Universität Bonn (2019), https://hdl.handle.net/20.500.11811/7868
[7] P. Kroenert et al., *Truncated partial-wave analysis for η-photoproduction observables via Bayesian statistics*, Submitted to Physical Review C (2023), https://doi.org/10.48550/arXiv.2305.10367
[8] V.L. Kashevarov, P. Ott, S. Prakhov, P. Adlarson, F. Afzal, Z. Ahmed, C.S. Akondi, J.R.M. Annand, H.J. Arends, R. Beck et al. (A2 Collaboration at MAMI), Phys. Rev. Lett. **118**, 212001 (2017)
[9] C.S. Akondi, J.R.M. Annand, H.J. Arends, R. Beck, A. Bernstein, N. Borisov, A. Braghieri, W.J. Briscoe, S. Cherepnya, C. Collicott et al. (A2 Collaboration at MAMI), Phys. Rev. Lett. **113**, 102001 (2014)
[10] O. Bartalini, V. Bellini, J. Bocquet, P. Calvat, M. Capogni, L. Casano, M. Castoldi, A. d'Angelo, J.P. Didelez, R. Di Salvo et al., The European Physical Journal A **33**, 169 (2007)
[11] F.N. Afzal, Ph.D. thesis, Rheinische Friedrich-Wilhelms-Universität Bonn (2019), https://hdl.handle.net/20.500.11811/8064
[12] F. Afzal et al. [A2 Collaboration], to be published soon
[13] J. Müller, J. Hartmann, M. Grüner, F. Afzal, A. Anisovich, B. Bantes, D. Bayadilov, R. Beck, M. Becker, Y. Beloglazov et al., Physics Letters B **803**, 135323 (2020)
[14] T. Bayes, Philosophical transactions of the Royal Society of London pp. 370–418 (1763)
[15] A. Gelman, J.B. Carlin, H.S. Stern, D.B. Dunson, A. Vehtari, D.B. Rubin, *Bayesian data analysis* (CRC press, 2013), https://doi.org/10.1201/b16018
[16] L. Tiator, M. Gorchtein, V.L. Kashevarov, K. Nikonov, M. Ostrick, M. Hadžimehmedović, R. Omerović, H. Osmanović, J. Stahov, A. Švarc, Eur. Phys. J. A **54**, 210 (2018), 1807.04525
[17] D. Rönchen, M. Döring, U.G. Meißner, C.W. Shen, *Light baryon resonances from a coupled-channel study including* $\mathbf{K\Sigma}$ *photoproduction* (2022), 2208.00089